Original Article

DAB2IP decreases cell growth and migration and increases sensitivity to chemotherapeutic drugs in colorectal cancer

Guanting Wu[1#], Xin Xu[2#], Daiwei Wan[1#], Diyuan Zhou[1], Yuan Feng[2], Junjie Chen[1], Zhijian Peng[3], Dong Fang[4], Xinyu Shi[1], Huihui Yao[1], Guoliang Chen[1], Liang Sun[1], Yizhou Yao[1], Guoqiang Zhou[5], Yili Yang[2,6], Songbing He[1]

[1]Department of General Surgery, the First Affiliated Hospital of Soochow University, Suzhou, China; [2]Suzhou Institute of Systems Medicine, Center for Systems Medicine, Chinese Academy of Medical Sciences, Suzhou, China; [3]Department of General Surgery, Kunshan Hospital of Traditional Chinese Medicine, Suzhou, China; [4]Department of Anorectal Surgery, Kunshan Hospital of Integrated Traditional Chinese and Western Medicine, Suzhou, China; [5]Department of Gastrointestinal Surgery, Changshu No. 2 Hospital, Suzhou, China; [6]China Regional Research Centre, International Centre of Genetic Engineering and Biotechnology, Taizhou, China

Contributions: (I) Conception and design: G Wu, Y Yang, S He; (II) Administrative support: X Xu, D Zhou, J Chen, L Sun, Y Yang; (III) Provision of study materials or patients: Z Peng, D Fang, G Zhou, Y Yang, S He; (IV) Collection and assembly of data: G Wu, X Shi, H Yao, G Chen, Y Yao; (V) Data analysis and interpretation: G Wu, X Xu, D Wan, Y Feng, S He; (VI) Manuscript writing: All authors; (VII) Final approval of manuscript: All authors.

[#]These authors contributed equally to this work.

Correspondence to: Songbing He. Department of General Surgery, the First Affiliated Hospital of Soochow University, Suzhou 215006, China. Email: captain_hsb@163.com; Guoqiang Zhou. Department of Gastrointestinal Surgery, Changshu No. 2 Hospital, Changshu 215123, China. Email: chowgq@sina.com.

Background: Colorectal cancer (CRC) is one of the most common cancers worldwide with high rates of invasiveness and mortality. DAB2IP (DOC2/DAB2 interactive protein) is a member of the RAS-GTPase-activating protein (RAS-GAP) family that shows a suppressive effect on cancer progression, is downregulated in several cancers. However, the role of DAB2IP in CRC remains elusive.

Methods: Expression of DAB2IP was evaluated in human CRC tissues using immunohistochemistry (IHC), quantitative real-time reverse transcription PCR (qRT-PCR) and immunoblotting. Knockdown and overexpression of DAB2IP in CRC cells were achieved by transfecting siRNAs and DAB2IP expression vectors and assessed by qRT-PCR and immunoblotting. CCK-8, colony formation, wound-healing, and transwell assays were used to evaluate CRC cell growth, migration, and sensitivity to chemotherapeutic drugs. The cell cycle was analyzed by propidium iodide (PI) staining and flow cytometry. Cell apoptosis was evaluated by Annexin V-DAPI double staining and flow cytometry. The effect of DAB2IP overexpression on tumor formation was explored by an *in vivo* tumorigenesis assay. Finally, immunoblotting was performed to examine the molecules related to the action of DAB2IP in CRC.

Results: Compared with para-cancer tissues, there was a marked decrease of DAB2IP expression in surgically excised CRCs. In cultured CRC cells, enforced expression of DAB2IP inhibited cell growth and migration and sensitized the cells to DNA-acting cisplatin, oxaliplatin, and doxorubicin but not 5-fluorouracil (5-FU). In contrast, knockdown of DAB2IP produced the opposite effect. Moreover, DAB2IP overexpression hindered tumor growth *in vivo*. We further found that DAB2IP regulated the expression of cell growth, epithelial-mesenchymal transition (EMT), and apoptosis-related proteins in CRC cells and inhibited the phosphorylation of protein kinase B (AKT) and extracellular signal-regulated kinase (ERK).

Conclusions: Expression of DAB2IP inhibited CRC cell growth and migration and sensitized CRC cells to chemotherapeutic drugs. Inhibition of the phosphorylation of AKT and ERK is associated with the effects of DAB2IP expression. Restoration of DAB2IP expression may be a novel target for treating CRC.

Keywords: Colorectal cancer (CRC); DAB2IP; cell growth; cell migration; chemosensitivity

Submitted Jun 10, 2021. Accepted for publication Aug 11, 2021.
doi: 10.21037/atm-21-3474
View this article at: https://dx.doi.org/10.21037/atm-21-3474

Introduction

Colorectal cancer (CRC) is the third most commonly diagnosed cancer, accounting for 9.7% of total global cases. It is the second most common cause of cancer deaths worldwide, with approximately 700,000 deaths annually (1-3). The incidence rate of CRC is increasing significantly in many developing regions, largely due to population aging, dietary changes, and environmental contamination (4). According to a recent cancer research, the incidence and morbidity of CRC in China have been up to 431,951 and 22.4 per 100,000 (5). Although radical resection combined with early diagnostic screening and comprehensive treatment have improved the clinical outcomes of CRC, approximately one-third of patients develop metastasis with a poor prognosis (6,7). Furthermore, the development of chemoresistance limits the effectiveness of chemotherapy in CRC. As such, there is an urgent need to identify an effective and sensitive biomarker that can predict prognosis and guide postoperative treatment for patients with CRC.

Disabled homolog 2 interacting protein (DAB2IP) is a member of the Ras GTPase-activating protein family located at chromosome 9q33.1–q33.3. It interacts with the tumor suppressor DAB2 and negatively regulates the Ras-mediated signaling pathway (8). Downregulation of DAB2IP has been found in several cancer types, such as bladder cancer, hepatocellular cancer, prostate cancer, and gastric cancer (9-12). Recent research also indicates that DAB2IP governs multiple tumor cellular biological processes, including cell growth, apoptosis, migration, and epithelial-mesenchymal transition (EMT) via several signaling pathways (13-16). In consistency, previous studies showed that DAB2IP was significantly downregulated in CRC tissues and absence of DAB2IP promoted CRC cell proliferation and migration (17,18). However, the potential role of DAB2IP in CRC cell tumorigenesis *in vivo* and the molecular mechanism of DAB2IP in CRC cell sensitivity to chemotherapy require further exploration.

In the present study, we further confirmed the low expression of DAB2IP in CRC and explored the effect of DAB2IP on CRC cell growth and migration. We provided the evidence that overexpression of DAB2IP increased sensitivity to chemotherapeutic drugs in colorectal cancer. We also demonstrated that DAB2IP could enhance apoptosis of CRC cells following cisplatin and reprogram a subset of apoptosis-related gene expression. Mechanistically, we revealed that DAB2IP could suppress the phosphorylation of ERK and AKT, which may be implicated in DAB2IP regulation of CRC cell chemosensitivity. These suggest that DAB2IP is a potent tumor suppressor in CRC and it may be likely to become an effective therapeutic target for the clinical treatment of CRC.

We present the following article in accordance with the ARRIVE reporting checklist (available at https://dx.doi.org/10.21037/atm-21-3474).

Methods

Patient specimens

Between 2016 and 2019, and without artificial selection, CRC tissues and adjacent para-cancer tissues were collected from patients diagnosed with CRC in the First Affiliated Hospital of Soochow University (Suzhou, China). Fifty pairs of samples were used for immunohistochemistry (IHC) and 16 pairs for qRT-PCR and immunoblotting analysis. The inclusion criteria were as follows: (I) diagnosed as colorectal cancer by postoperative pathological analysis with no prior history of cancer; (II) patients have not undergone any type of preoperative therapy, including neoadjuvant chemotherapy, radiotherapy, or other therapy; (III) patients agreed to be followed up with unabridged clinical data; (IV) patients were informed about the details of the study and signed informed consent. All procedures performed in this study involving human participants were in accordance with the Declaration of Helsinki (as revised in 2013). The study was approved by Biomedical Research Ethics Committee of the First Affiliated Hospital of Soochow University (Suzhou, China) (2021-NO:177) and informed consent was taken from all the patients.

IHC

Expression of DAB2IP in tumor tissues and adjacent normal

Table 1 Summarize of siRNAs and primers sequences used in this study

Name	Sequence
FAM NC sense	5'-UUCUCCGAACGUGUCACGUTT-3'
FAM NC antisense	5'-ACGUGACACGUUCGGAGAATT-3'
siDAB2IP-1 sense	5'-GGGAUAGGCUAAGGAGUAATT-3'
siDAB2IP-1 antisense	5'-UUACUCCUUAGCCUAUCCCTT-3'
siDAB2IP-2 sense	5'-CUGGAGCAGAGCAUAGUAUTT-3'
siDAB2IP-2 antisense	5'-AUACUAUGCUCUGCUCCAGTT-3'
siDAB2IP-3 sense	5'-CGCUGUAUGAGUCAGAUGATT-3'
siDAB2IP-3 antisense	5'-UCAUCUGACUCAUACAGCCTT-3'
DAB2IP forward primer	5'-CTGAGCGGGATAAGTGGATGG-3'
DAB2IP reverse primer	5'-AAACATTGTCCGTCTTGAGCTT-3'
GAPDH forward primer	5'-GGAGCGAGATCCCTCCAAAAT-3'
GAPDH reverse primer	5'-GGCTGTTGTCATACTTCTCATGG-3'

tissues was examined by IHC. Tissues were formalin fixed and paraffin embedded and then cut into 5 μm sections. The sections were dewaxed in xylene twice and rehydrated using graded ethanol, then incubated with 30% hydrogen peroxide for 10 minutes to block the endogenous peroxidase. Next, the sections were incubated with goat serum for 30 minutes, then the goat serum was removed, and DAB2IP antibodies (Abcam, Cambridge, England) were added overnight at 4 ℃. The slides were washed with distilled water three times for 10 minutes each, incubated with secondary antibodies for 30 minutes, and then washed with distilled water three times for 10 minutes each. Finally, the sections were colored with diaminobenzidine after washing. The expression of DAB2IP was evaluated by the ratio of positive cells and the intensity of staining. The immunoreactive scores (IRSs) were the product of the percentage of positive cells (0, <5%; 1, 5–25%; 2, 25–50%; 3, 50–75%; 4, >75%) multiplied by the staining intensity (0, negative; 1, weak; 2, moderate; 3, strong). The IRS was then classified as negative [0–1], weakly positive [2–3], moderately positive [4–7], or strongly positive [8–12]. The IHC results were evaluated by two pathologists separately.

Cell culture and reagents

The human CRC cell lines including HCT116, SW480, LOVO, and RKO were purchased from American Type Culture Collection, Maryland, USA. The human embryonic kidney HEK293T cell line was kindly provided by Dr. Kunkun Han from The Asclepius Technology Company Group and Asclepius Cancer Research Center, Suzhou, Jiangsu, China. Cells were cultured in Dulbecco's Modified Eagle Medium (DMEM) (Hyclone, Los Angeles, CA, USA) supplemented with 10% fetal calf serum (Gibco, Grand Island, NY, USA) and 1% penicillin/streptomycin (Gibco, Grand Island, NY, USA). All cells were cultured at 37 ℃ in a 5% CO_2 humidified atmosphere. The human CRC cell lines were treated with different concentrations of cisplatin (Selleckchem, Huston, TX, USA), doxorubicin (DOX) (Selleckchem, Huston, TX, USA), oxaliplatin (Selleckchem, Huston, TX, USA), and 5-fluorouracil (5-FU) (Selleckchem, Huston, TX, USA) to evaluate the effects of DAB2IP on the drug sensitivity of CRC cells.

siRNA oligonucleotides, plasmids, lentivirus, and cell transfection

One FAM NC siRNA (siNC) oligonucleotide and three different pairs of DAB2IP-specific siRNA oligonucleotides (siDAB2IP-1, siDAB2IP-2, and siDAB2IP-3) were designed and purchased from Sangon Biotech (Shanghai, China). Sequences of siRNAs used in this study are listed in *Table 1*. Human DAB2IP cDNA was generated and cloned into a pcDNA3.1 vector with a Flag tag (gifts from Dr. Xin Xu, Suzhou Institute of Systems Medicine, Suzhou, Jiangsu, China). Plasmids or siRNAs were transiently transfected into HCT116 cells by Lipofectamine 2000 (Invitrogen, Carlsbad, CA, USA) or Lipofectamine RNAiMAX (Invitrogen, Carlsbad, CA, USA) according to the manufacturer's instructions. Human DAB2IP cDNA was also generated and cloned into a pLVX-Puro vector (Fenghui Biotechnology, #BR025, Hunan, China). For lentiviral packaging, the recombinant vectors were transfected with the psPAX2 lentivirus-packaged vector and the PMD2G lentivirus-envelope plasmid (gifts from Dr. Xiaodan Hou, Suzhou Institute of Systems Medicine, Suzhou, Jiangsu, China) in HEK293T cells by using polyethylenimine (Sigma-Aldrich, Missouri, USA) according to the manufacturer's instructions. Lentivirus particles were transfected into the HCT116 cells in the presence of 6 μg/mL polybrene. Stable cell lines for subcutaneous injection were further selected with 0.5 μg/mL puromycin (Sigma-Aldrich, Missouri, USA) for 2 weeks.

Table 2 Summarize of antibodies information used in this study

Name	Company	Catalog number	Antibody concentration
DAB2IP	Abcam	ab87811	1:1,000 or 1:500
Flag	Medical & Biological Laboratories	M185-3L	1:2,000
P53	Cell Signaling Technology	2527	1:1,000
P21	Cell Signaling Technology	2947	1:1,000
Cyclin D1	Cell Signaling Technology	55506	1:1,000
CDK4	Cell Signaling Technology	12790	1:1,000
ZO-1	Cell Signaling Technology	8193	1:1,000
Claudin-1	Cell Signaling Technology	13255	1:1,000
β-Catenin	Cell Signaling Technology	8480	1:1,000
Snail	Cell Signaling Technology	3879	1:1,000
E-Cadherin	Cell Signaling Technology	3195	1:1,000
PARP	Cell Signaling Technology	9532	1:1000
P-AKT	Cell Signaling Technology	4060	1:1,000
AKT	Cell Signaling Technology	4691	1:1,000
P-ERK	Cell Signaling Technology	4370	1:1,000
ERK	Cell Signaling Technology	4695	1:1,000
Bcl-xL	Bimake	A5091	1:1,000
Bcl-2	Bimake	A5010	1:1,000
GAPDH	Abgent	AM1020b	1:2,000

Bioinformatics analysis

Data on 10 CRC tissues from patients with liver metastasis (s1_2_NS-s10_2_NS) and 10 CRC tissues from patients without liver metastasis (s1_1_NS-s10_1_NS) were retrieved from the human mRNA microarray GSE147603 in the Gene Expression Omnibus (GEO) database (https://www.ncbi.nlm.nih.gov/geo). To predict the potential downstream signaling pathway of DAB2IP expression in CRC and further understand the biological process of DAB2IP expression, we performed a gene set enrichment analysis (GSEA). The GSEA was conducted to investigate pathways enriched in the high DAB2IP expression and low DAB2IP expression subgroups. The gene expression data for CRC were obtained from the KEGG database. The differential gene expression analyses and GSEA were performed using R software.

Immunoblotting analysis

Total cell lysates were prepared using RIPA lysis buffer (Beyotime Biotechnology Institute) and quantified using a BCA protein quantification kit (Beyotime Biotechnology Institute) according to the manufacturer's protocols. Whole proteins were separated by SDS-PAGE and transferred to PVDF membranes, then blocked with 5% non-fat milk for 1 hour at room temperature. The membranes were then probed with the selected primary antibodies at 4 ℃ with gentle shaking overnight and incubated with corresponding horseradish peroxidase-(HRP-) conjugated secondary antibodies. Antibodies used in this study are listed in *Table 2*. The Horseradish peroxidase-conjugated anti-mouse and anti-rabbit IgG antibodies were purchased from Beyotime Biotechnology (Nantong, China). Blots were detected at ChemiDoC

MP system (Bio-Rad Laboratories Inc., CA, USA) using Tanon™ High-sig ECL peroxide reagent (Tanon, Shanghai, China). The bands were generated using ImageLab (Bio-Rad Laboratories Inc., CA, USA) and then quantified using ImageJ (NIH, USA).

Quantitative real-time polymerase chain reaction (qRT-PCR)

Total RNA was extracted from cells and tissues using Trizol (Takara Bio Group, Japan), and 1 μg of RNA was added to synthesize cDNA using the PrimeScript™ RT reagent Kit with gDNA Eraser (Takara Bio Group, Otsu, Japan) according to the manufacturer's instructions. qRT-PCR was performed with SYBR Green qPCR Master Mix (Takara Bio Group, Otsu, Japan) using the Roche LightCycler® 480II real-time PCR system (Roche, Basel, Switzerland) to evaluate the efficiency of the selected DAB2IP siRNAs and plasmids. Primers used in this study are listed in *Table 1*.

Cell growth and viability

The HCT116 cells were transfected with selected siRNAs or an increased amount of plasmids, then seeded in 96-well plates at a start density of 4,000 cells per well. After culturing for an additional 1–4 days, cell viability was evaluated by CCK-8 staining according to the manufacturer's instructions (Bimake Houston, TX, USA). After transfection, the cells were also plated at a start density of 6,000 cells per well into 96-well plates for 1 day before cisplatin, oxaliplatin, DOX, and 5-FU treatment. Then the cells were incubated for 24 hours with different concentrations of cisplatin, oxaliplatin, DOX, and 5-FU. CCK-8 solution was added to each well for 1–4 hours. A SpectraMax iX3 microplate reader (Molecular Devices, CA, USA) was employed to measure the absorbance at 450 nm. Cell viability was calculated and presented as the change of relative absorbance in percentage.

Cell cycle analysis

HCT116 cells were transfected with selected plasmids or siRNAs and cultured in DMEM containing CS-FBS for 24 hours. The cells were harvested 3 days later and fixed with 75% ice-cold ethanol for 16 hours at 4 ℃. Then the cells were washed and suspended with ice-cold PBS and incubated with 100 mg/mL RNase and 40 mg/mL propidium iodide (PI) (BD Pharmingen, San Diego, USA) for 30 minutes at room temperature. The results were detected by Attune NxT flow cytometry (Life Technologies, Thermo Fisher Scientific, MA, USA) and analyzed with FlowJo (Version 10).

Colony formation assay

After transfection with selected siRNAs or an increased number of plasmids, 1,000 HCT116 cells were placed in 6-well plates for 10 days and then fixed and stained with 0.1% crystal violet. The number of foci containing >100 cells was determined at 40× magnification using an optical microscope (Biocentury, China), and the images were taken by a digital camera (Leica, Germany).

In vivo tumorigenicity assay

BALB/c nude mice (SPF grade, 18–22 g, 8 weeks old, male) were purchased from Shanghai SLRC Laboratory Animal Co., Ltd. (Shanghai, China). CRC cell xenografts were performed on the BALB/C nude mice. A total of 5×10^6 NC-OE or DAB2IP-OE HCT116 cells (NC, DAB2IP) were suspended in 100 μL of serum-free DMEM medium and inoculated subcutaneously in the flank of the nude mice (n=10, 5/group). Tumor volumes were measured at 7, 10, 14, 17, and 21 days after implantation and were calculated using the formula: volume = (length × width^2)/2. At the end of the experiment, the nude mice were euthanized, and the tumors were excised, weighed, and subjected to other experiments. Experiments were performed under a project license (No. ISM-IACUC-0054-R) granted by Animal Ethics Committee of Suzhou Institute of Systems Medicine (Suzhou, China), in compliance with institutional guidelines for the care and use of animals. A protocol was prepared before the study without registration.

Cell migration assay

A wound-healing assay was performed as described below to test the migration ability of the CRC cells after transfection. The wounds were made in confluent monolayer cells using 10 μL pipette tips, and the culture was changed to a serum-free medium. Wound healing was detected at 0, 12, 24, and 36 hours within the scraped lines, and representative fields were photographed at the different time points. For the Transwell assay, 24-well Transwell plate without Matrigel (8 μm, Corning Incorporated, USA) was used to detect the migration ability of HCT116 cells. After transfection

(1×10^5 cells/well), the HCT116 cells were suspended in 200 µL of serum-free medium and placed in the upper compartment of each chamber, then 800 µL of culture medium with 10% serum was added to the lower chamber as a chemoattractant. Cells were allowed to migrate for 24 hours at 37 ℃. Cells on the upper side of the insert filter were completely removed by wiping with a cotton swab, and the filters were fixed with 4% paraformaldehyde. Then, cells were stained with 0.1% crystal violet solution. Cells were observed and imaged using an optical microscope (Biocentury, China).

Cell apoptosis assay

HCT116 CRC cells (6×10^5 cells/well) were seeded in 6-well plates. After overnight incubation, the cells were transfected with selected siRNAs or plasmids and cultured in DMEM containing CS-FBS for 24 hours. Then the media were aspirated, and new media containing different concentrations of several indicated chemotherapeutics, including cisplatin, oxaliplatin, DOX, and 5-FU were added for overnight treatment. Subsequently, the cells were washed with PBS and suspended in 500 µL of binding buffer, including 5 µL annexin V-FITC and 3 µM DAPI for 15 minutes at room temperature in the dark. Annexin V-FITC was purchased from Beyotime Biotechnology (Nantong, China). DAPI was purchased from Biolegend (San Diego, USA). The results were detected by Attune NxT flow cytometry (Life Technologies, Thermo Fisher Scientific, MA, USA) and analyzed with FlowJo (Version 10).

Statistical analysis

All experiments were conducted in triplicate technical replicates, and all data are presented as mean ± standard error of the mean (SEM). Statistical significance was determined by Student's *t* test or one-way ANOVA using GraphPad Prism (Version 7.0, USA). A value of $P<0.05$ was used to indicate a statistically significant difference.

Results

Decreased DAB2IP expression in primary CRCs

Given that DAB2IP functions as a tumor suppressor in many cancers, we firstly evaluated the expression of DAB2IP using the public GEPIA RNAseq and Oncomine databases that are based on TCGA database and we confirmed that DAB2IP expression was significantly lower in colorectal adenocarcinoma and rectum adenocarcinoma than in normal controls (*Figure 1A*). To determine whether DAB2IP has a role in the oncogenic process of CRC, we used IHC staining to compare DAB2IP expression in 50 paired tissue samples collected from para-cancer tissues and tumor tissues. Notably, the results showed the expression of DAB2IP was significantly lower in the primary CRC tissues. By contrast, abundant DAB2IP expression was present in the matched normal tissues (*Figure 1B,1C*). A significantly reduced DAB2IP mRNA level and protein level in cancerous tissues were confirmed by qRT-PCR and immunoblotting analysis in 16 paired CRC tissues (*Figure 1D-1F*).

Transient knockdown and overexpression of DAB2IP in CRC cells

To further investigate the potential role of DAB2IP in the development of CRC, immunoblotting was used in the present study to examine DAB2IP expression in four CRC cell lines, including HCT116, SW480, RKO, and LOVO. Our results revealed that HCT116 cells expressed a higher level of DAB2IP among four CRC cell lines (*Figure 2A*). We then used the HCT116 cells for further studies. To explore the molecular mechanism of DAB2IP involved in the progression of CRC, DAB2IP was transiently knocked down using three different siRNAs in the HCT116 cell line with a high endogenous DAB2IP level, and the knockdown efficiency was confirmed by immunoblotting and qRT-PCR analysis. Results from immunoblotting and qRT-PCR showed that DAB2IP expression at both the protein and mRNA levels was significantly decreased in cells transfected with siRNAs targeting DAB2IP (siDAB2IP-1, siDAB2IP-2, and siDAB2IP-3) compared with cells transfected with FAM NC siRNA (siNC) (*Figure 2B*). We also transiently overexpressed DAB2IP by transfecting Flag-DAB2IP-pcDNA3.1 plasmids into HCT116 cells. The overexpression efficiency of DAB2IP was confirmed by immunoblotting and qRT-PCR analysis. Our results showed that both DAB2IP protein and mRNA expression levels were notably higher in cells transfected with plasmids encoding human DAB2IP (Flag-DAB2IP) than in cells transfected with an empty vector (Flag-pcDNA3.1) (*Figure 2C*).

Characteristics and correlated functions of DAB2IP in CRC progression

Since DAB2IP expression was downregulated in CRC

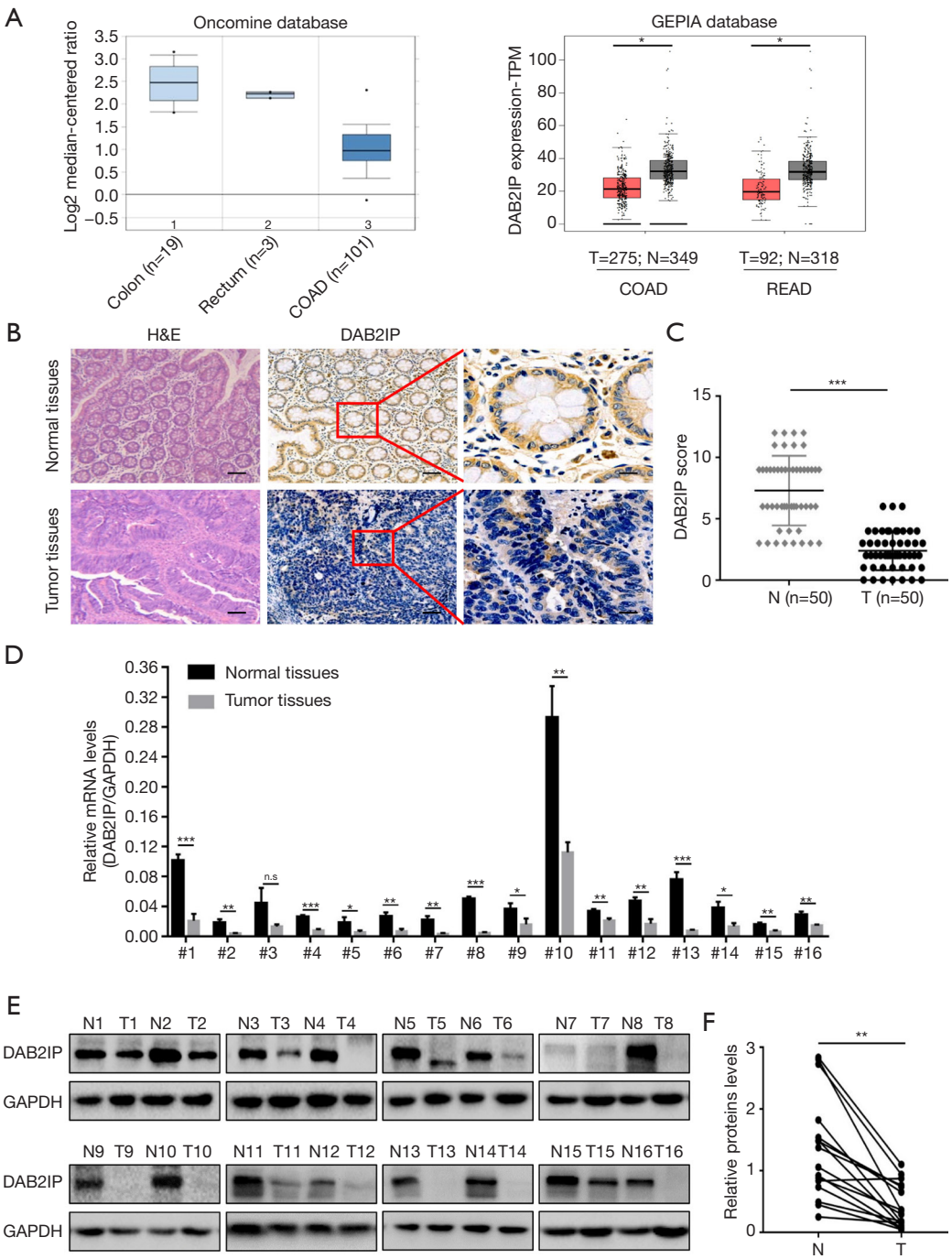

Figure 1 Decreased DAB2IP expression in primary colorectal cancers. (A) Differences in DAB2IP gene expression between CRC and normal samples observed from two published databases (Oncomine and GEPIA). (B) Immunohistochemical (IHC) staining of DAB2IP in representative carcinoma and the surrounding normal tissues of colorectal cancer (scale bar =100 μm). (C) Scatter plot analysis of DAB2IP levels in 50 colorectal cancer tumors (T) and paired normal tissues (N). (D) qRT-PCR analysis of DAB2IP mRNA level in 16 randomly selected pairs of CRC tumors and surrounding normal tissues. (E) Immunoblotting analysis of DAB2IP protein in 16 randomly selected pairs of CRC tumors (T) and surrounding normal tissues (N). (F) Quantification analysis of DAB2IP expression with GAPDH as a loading control. *, P<0.05; **, P<0.01; ***, P<0.001.

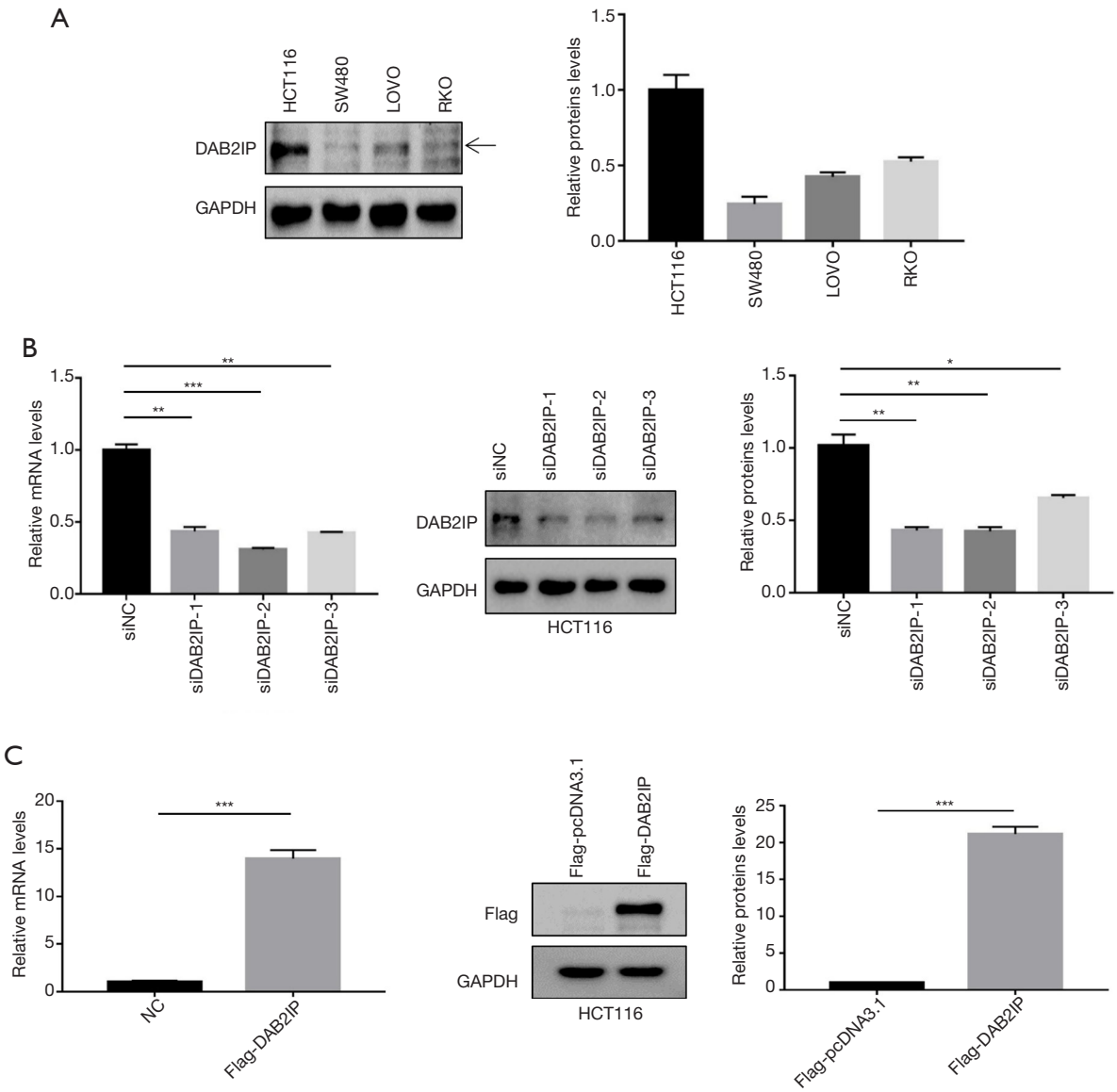

Figure 2 Transient knockdown and overexpression of DAB2IP in CRC cells. (A) The expression of DAB2IP in four CRC cell lines (HCT116, SW480, LOVO, and RKO). The gray-scale value of straps visually shows the expression of DAB2IP in the cell lines (Image J software). Error bars represent SEM (n=3). (B) The protein and mRNA levels of DAB2IP expression in cells transfected with FAM NC (siNC) and in cells transfected with three different siRNAs against DAB2IP (siDAB2IP-1, siDAB2IP-2, and siDAB2IP-3) tested by immunoblotting and qRT-PCR using HCT116 cells. The gray-scale value of straps visually shows the expression of DAB2IP in the cell lines (Image J software). Error bars represent SEM (n=3). (C) The protein and mRNA levels of Flag and DAB2IP expressions in cells transfected with Flag-pcDNA3.1 plasmids (Flag-pcDNA3.1) and cells transfected with Flag-DAB2IP-pcDNA3.1 plasmids (Flag-DAB2IP) tested by immunoblotting and qRT-PCR. The gray-scale value of straps visually shows the expression of Flag in the cell lines (Image J software). Error bars represent SEM (n=3). *, P<0.05; **, P<0.01; ***, P<0.001.

tissues, we were interested to know whether DAB2IP expression has a causal role in regulating CRC cell phenotypes and the role DAB2IP plays in CRC. We compared 10 primary CRC tissues without liver metastasis and 10 primary CRC tissues with liver metastasis using mRNA microarray. A total of 236 genes were dysregulated in the primary tumor tissues with liver metastases, of which 74 genes were upregulated and 162 downregulated. These 236 differentially expressed genes are shown by hierarchical clustering and volcano plot. We found that DAB2IP expression was significantly lower in metastasis-related CRC tissues than in primary CRC tissues (*Figure 3A,3B*). A GSEA was used to predict the potential downstream signaling pathway and correlated functions of DAB2IP expression in CRC progression. The GSEA results showed that DAB2IP expression was correlated with the cell cycle, DNA replication, focal adhesion, ECM-receptor interaction, Hedgehog signaling pathway, Wnt signaling pathway, Neurotrophin signaling pathway, melanogenesis, and regulation of Actin cytoskeleton (*Figure 3C*). These correlated functions of DAB2IP provided directions for our follow-up research.

Overexpression of DAB2IP inhibited CRC cell growth and induced cell cycle arrest via the P53/P21 pathway

Since the bioinformatics analysis showed that DAB2IP expression was correlated with cell cycle, DNA replication, and focal adhesion, we verified these findings with further experiments. CCK-8 assays were used to analyze the effect of DAB2IP on the growth of CRC cells. We found the proliferation rate of DAB2IP knockdown cells was significantly higher, and the proliferation rate of DAB2IP overexpressed cells was significantly lower compared to the negative controls (*Figure 4A*). These results demonstrated a link between DAB2IP expression and CRC cell growth. Therefore, we next sought to explore the underlying mechanisms of DAB2IP in this event. Immunoblotting results revealed that upregulation of DAB2IP decreased the expression level of cyclin D1 and CDK4, while downregulation of DAB2IP showed the opposite effect (*Figure 4B,4C*). Consistent with the CCK-8 assay results, colony formation assay results found that DAB2IP knockdown cells showed an enhanced colony-formation ability that was markedly suppressed in the DAB2IP overexpressed cells (*Figure 4D*) confirming the inhibitory effect of DAB2IP in CRC cell growth. Analogously, to investigate the effect of DAB2IP on the cell cycle in HCT116 cells, we used flow cytometry to monitor the percentage of cells which were in each different mitotic phase. Our results showed that after transfection with selected siRNAs, DAB2IP knockdown increased the percentage of cells in G2/M phase. Meanwhile, the percentage of cells in the G0/G1 and S phases was decreased in a certain extent. Cells with overexpressed DAB2IP showed the opposite effect (*Figure 4E,4F*). In addition, to understand the underlying mechanisms of DAB2IP in this phenomenon, HCT116 cells transfected with selected siRNAs or plasmids were analyzed by immunoblotting for P53 and P21 expression levels, which are both closely associated with cancer cell cycle arrest. Collectively, our results found that DAB2IP overexpression notably increased the P53 and P21 expression levels in HCT116 cells. In contrast, knockdown of DAB2IP had the opposite effect on P53 and P21 expression levels (*Figure 4G*).

DAB2IP overexpression inhibited tumor growth in CRC in vivo

For confirmation, we next evaluated the role of DAB2IP in CRC tumorigenesis *in vivo* with a subcutaneous tumor experiment in mice. Compared to the NC group, DAB2IP overexpression significantly inhibited CRC tumor volume, size, and weight (*Figure 5A-5C*). As shown in *Figure 5D* and *5E*, qRT-PCR and immunoblotting confirmed that DAB2IP overexpression resulted in upregulation of DAB2IP mRNA and protein levels in the subcutaneous tumors from nude mice. This indicated that DAB2IP overexpression inhibited the tumor growth both *in vivo* and *in vitro*.

Ectopic DAB2IP inhibited the migration and EMT progress of CRC cells

To elaborate on the effect mechanism of DAB2IP on CRC cells, we evaluated the migration ability of CRC cells after they were knocked down or overexpressed using selected siRNAs or plasmids. First, healing wound assays were applied to measure the effect of DAB2IP on the migration of HCT116 cells. Our results showed that DAB2IP loss potentiated the motility of HCT116 cells and DAB2IP overexpression restrained this phenomenon (*Figure 6A-6C*). Furthermore, for confirmation, we evaluated the migration ability of CRC cells via a transwell assay after cells were transfected with selected siRNAs or plasmids. Compared with the negative controls, the migration ability of DAB2IP knockdown HCT116 cells increased. However,

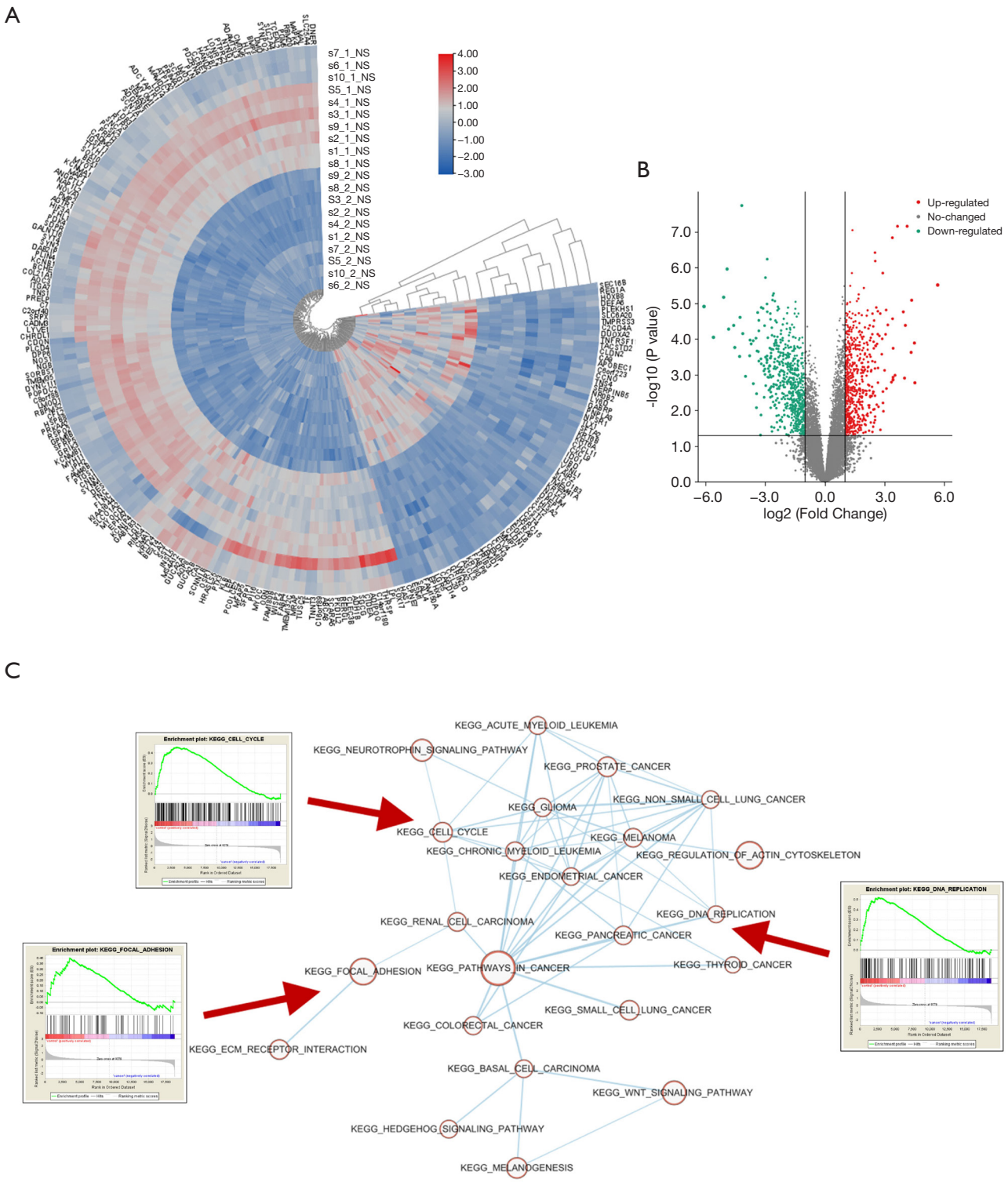

Figure 3 Characteristics and correlated functions of DAB2IP in CRC progression. (A,B) The gene expression profiles of 10 primary CRC tumors without liver metastasis and 10 primary tumor tissues with liver metastasis using mRNA microarray, with 236 dysregulated genes identified by hierarchical clustering and volcano plot. (C) GSEA analysis shows that cell cycle, DNA replication, and focal adhesion are closely correlated with DAB2IP.

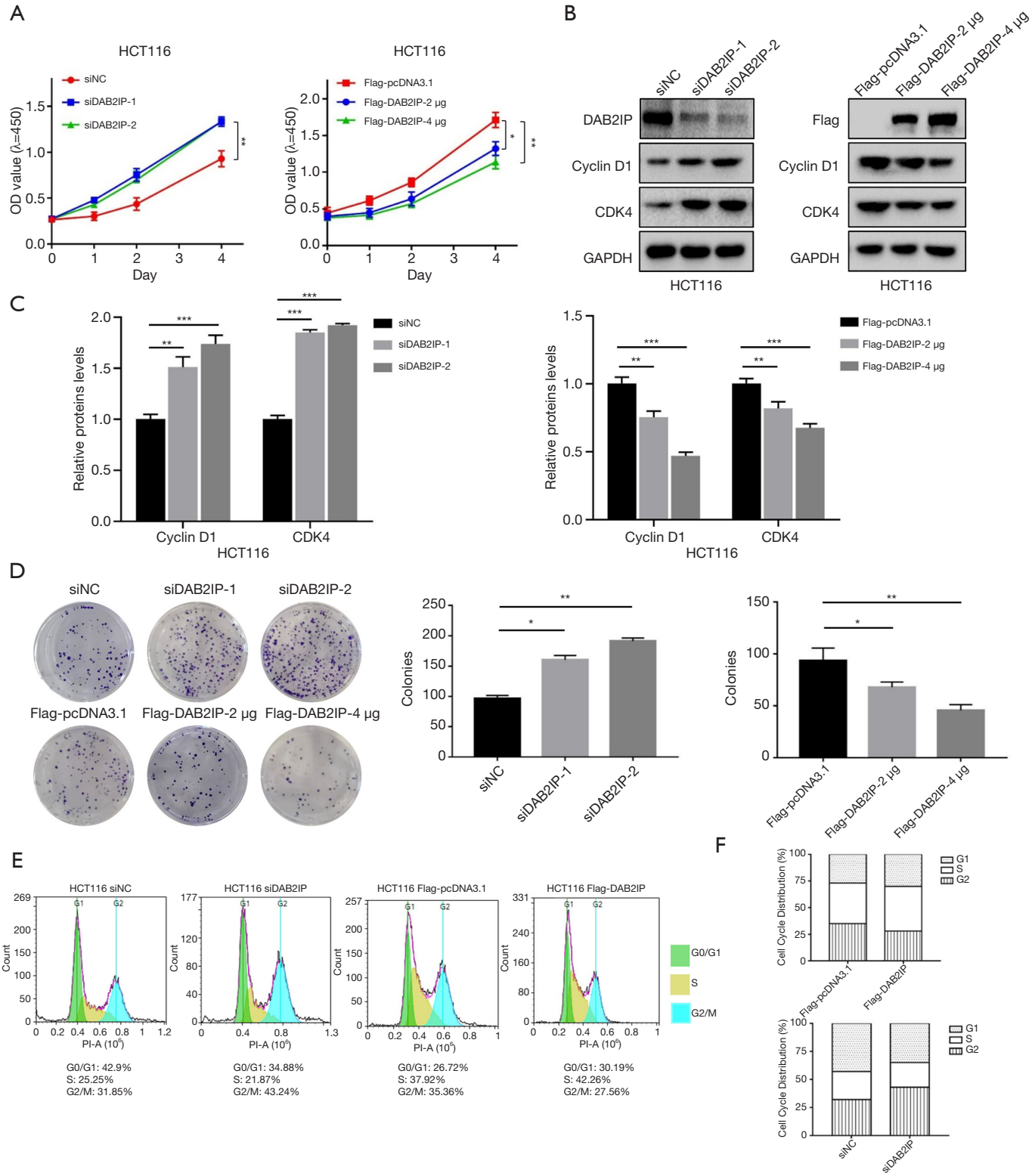

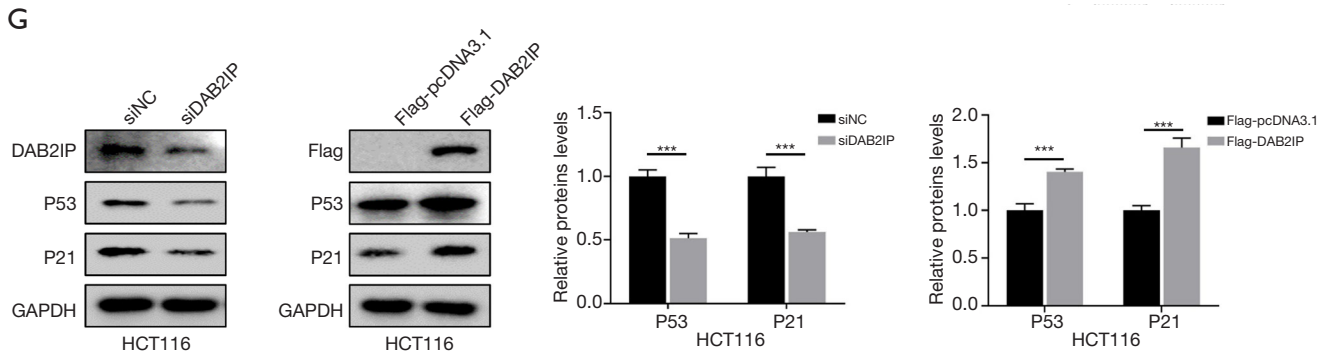

Figure 4 Overexpression of DAB2IP inhibits CRC cell growth and induces cell cycle arrest via the P53/P21 pathway. (A) Results of CCK8 assays used to test the proliferation ability of HCT116 cells transfected with selected siRNAs (siNC, siDABIP-1, and siDAB2IP-2) or increased amounts of plasmids (Flag-pcDNA3.1, Flag-DAB2IP-2 μg, and Flag-DAB2IP-4 μg) for 24 hours, presented as mean ± SEM (n=6). (B,C) After transfection with selected siRNAs (siNC, siDAB2IP-1, and siDAB2IP-2) or increased amounts of plasmids (Flag-pcDNA3.1, Flag-DAB2IP-2 μg, and Flag-DAB2IP-4 μg) for 24 hours, HCT116 cells were analyzed for DAB2IP, Flag, Cyclin D1, and CDK4 levels by immunoblotting with GAPDH as the loading control. The gray-scale value of straps visually shows the expression of Cyclin D1 and CDK4 in HCT116 (Image J software). Error bars represent SEM (n=3). (D) HCT116 cells transfected with selected siRNAs (siNC, siDAB2IP-1, and siDAB2IP-2) or increased amounts of plasmids (Flag-pcDNA3.1, Flag-DAB2IP-2 μg, and Flag-DAB2IP-4 μg) were maintained in culture media for 10 days and then fixed and stained with 0.1% crystal violet, and the colonies containing over 100 cells were counted manually. The representative photographs are presented (magnification, ×1), and the relative number of colonies counted. (E) Flow cytometry was performed to detect cell cycle after cells were transfected with selected siRNAs (siNC and siDAB2IP) or plasmids (Flag-pcDNA3.1 and Flag-DAB2IP) for 24 hours. (F) is the cartogram of (E). (G) After transfection with selected siRNAs (siNC and siDAB2IP) or plasmids (Flag-pcDNA3.1 and Flag-DAB2IP) for 24 hours, HCT116 cells were analyzed for DAB2IP, Flag, P53, and P21 levels by immunoblotting with GAPDH as the loading control. The gray-scale value of straps visually shows the expression of P53 and P21 in HCT116 (Image J software). Error bars represent SEM (n=3). *, P<0.05; **, P<0.01; ***, P<0.001.

the migration ability of DAB2IP overexpressed HCT116 cells decreased distinctly (*Figure 6D,6E*). Since DAB2IP is involved in CRC cell metastasis, it is possible that DAB2IP may regulate the progress of EMT. To test this, the expression of the epithelial marker E-cadherin and other proteins closely correlated with EMT progress, including ZO-1, Claudin-1, Snail, and β-Catenin were analyzed using immunoblotting analysis. Our results found that DAB2IP overexpression increased E-cadherin, ZO-1, and Claudin-1 expression but decreased Snail and β-Catenin expression. Conversely, knockdown of DAB2IP had the opposite effect (*Figure 6F*). Taken together, these results suggest that DAB2IP acts as a tumor suppressor in CRC cells, and its ectopic expression inhibits the migration and EMT progress of CRC cells *in vitro*.

DAB2IP regulated the drug sensitivity of cisplatin, oxaliplatin, and DOX on CRC cells and the intrinsic apoptosis of CRC cells following cisplatin administration

CRC is almost always diagnosed at an advanced stage when tumor cell dissemination has taken place. Unfortunately, chemotherapies provide only a limited increase in overall survival for these patients. A major reason for this clinical outcome is therapy resistance, with escape mechanisms to chemotherapy remaining the main culprits. The effect of DAB2IP on CRC cells propelled us to explore its impact on the cell sensitivity of several DNA-acting chemotherapeutic drugs which are commonly used in clinical settings, including cisplatin, oxaliplatin, DOX, and 5-FU. Using CCK-8 assays, our results showed that the presence of DAB2IP in HCT116 cells increased CRC cell sensitivity to cisplatin, oxaliplatin, and DOX but not to 5-FU (*Figure 7A*). It is known that cisplatin can induce apoptosis of CRC cells, and DAB2IP coordinates both PI3K-Akt and ASK1 pathways for cell survival and apoptosis (19,20). However, whether DAB2IP affects the apoptotic cell death of CRC cells after cisplatin treatment is still unknown. We therefore examined whether DAB2IP has effects on cisplatin-induced apoptosis of CRC cells. Indeed, as measured by flow cytometry, the percentage of apoptotic cells was significantly higher in DAB2IP overexpressed cells compared with

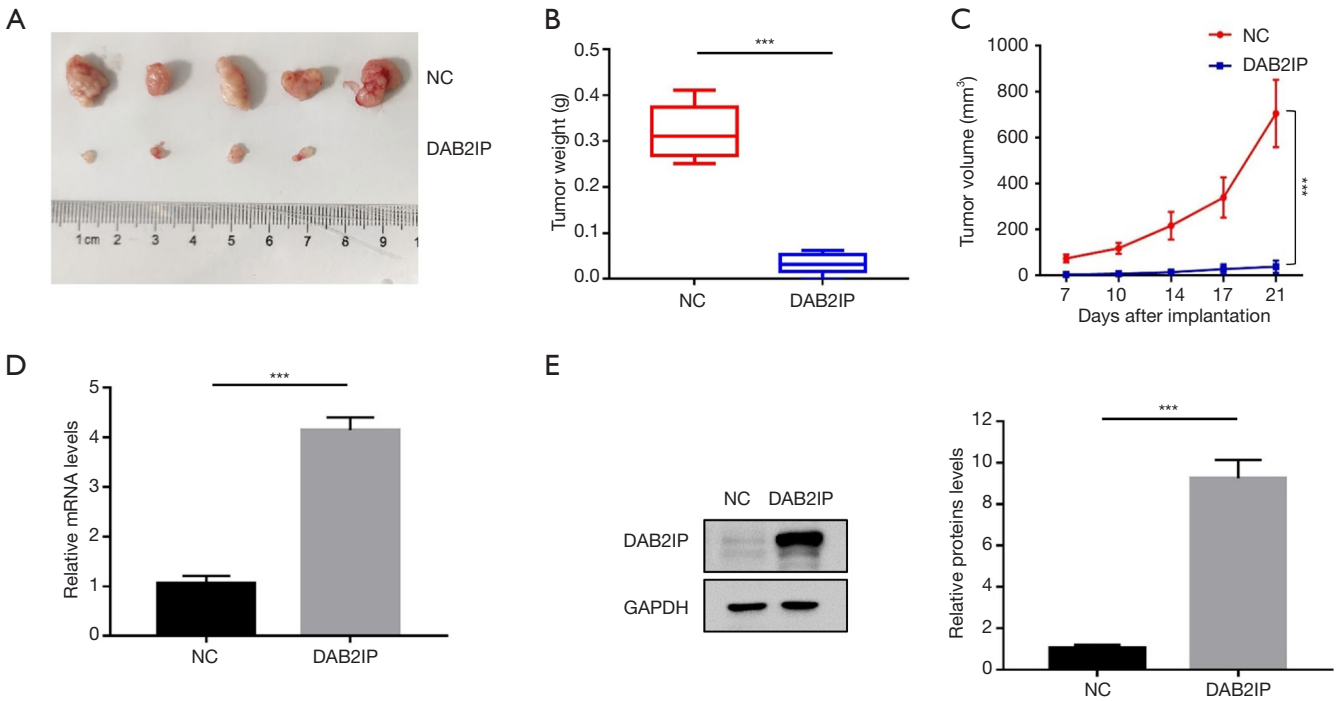

Figure 5 DAB2IP overexpression inhibits tumor growth in CRC *in vivo*. (A) Images of tumors taken from both groups 21 days after implantation. Tumors derived from the DAB2IP overexpressed (DAB2IP) HCT116 cells are significantly smaller compared with the NC group (NC). (B,C) The tumor weights and volumes as measured and recorded in both groups. (D,E) The qRT-PCR and immunoblotting analysis of DAB2IP mRNA and protein levels from the subcutaneous tumors of nude mice with GAPDH as the loading control. ***, P<0.001.

negative controls (*Figure 7B*,*7C*). Consistently, elevated cleaved subunits of PARP and decreased anti-apoptotic proteins, including Bcl-2 and Bcl-xL, were detected in cells that overexpressed DAB2IP following cisplatin treatment (*Figure 7D*). To dissect the possible mechanism of DAB2IP in this event, we explored possible downstream signaling pathways such as AKT and ERK, which are both closely associated with cancer cell apoptosis. Our results confirmed the inhibitory effect of DAB2IP on the AKT and ERK signaling pathways. We found that DAB2IP overexpression notably decreased the levels of phosphorylated AKT and phosphorylated ERK in HCT116 cells but not the total protein levels, and knockdown of DAB2IP had the opposite effect (*Figure7E*,*7F*).

Discussion

Due to the significant risk of recurrence and metastasis in CRC, there is a strong imperative to discover novel molecules from diverse biological sources that may elaborate the occurrence and progression of this epithelium-derived tumor. Clarifying and understanding the mechanisms of CRC development will help to develop new therapeutic strategies and improve CRC patient survival. DAB2IP, also named ASK1-interacting protein 1 (AIP1), is a member of the RAS-GTPase-activating protein (RAS-GAP) family and is downregulated in several cancer types, including bladder cancer, hepatocellular cancer, prostate cancer, gastric cancer, breast cancer, lung cancer, and pancreatic cancer (9-12,21-23). An increasing number of studies report that DAB2IP acts as a crucial tumor suppressor and plays a vital role in different aspects of biological activities, including cell apoptosis and survival, EMT, cancer stem cell phenotype, radiation resistance, DNA repair, and autophagy (20,24-27). However, there is a disparate view that upregulation of DAB2IP contributes to tumor development and growth in cutaneous squamous cell carcinoma, which means DAB2IP may also be a potential oncogene (28). These findings suggest that DAB2IP has become an attractive target for cancer therapy in recent years.

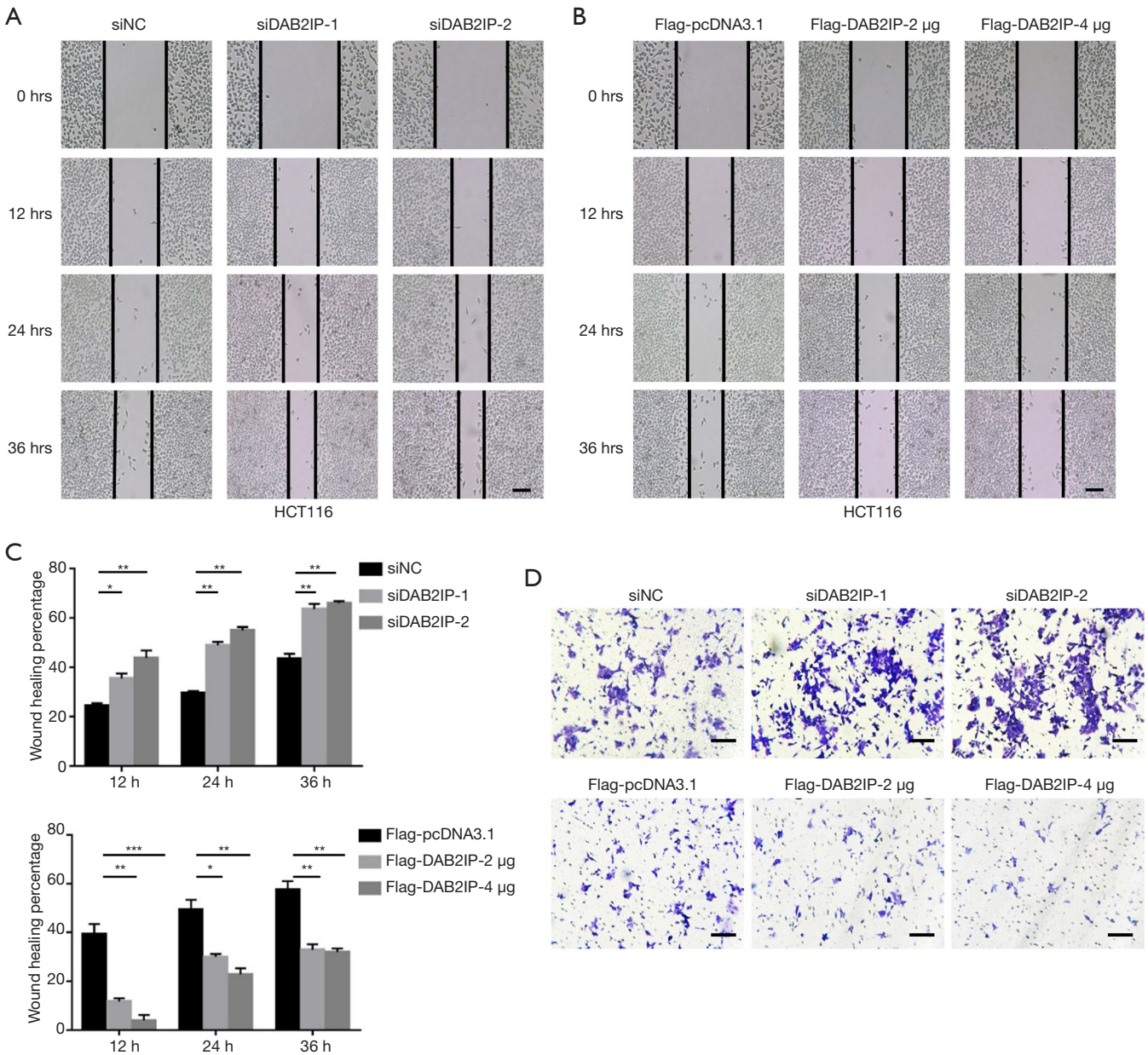

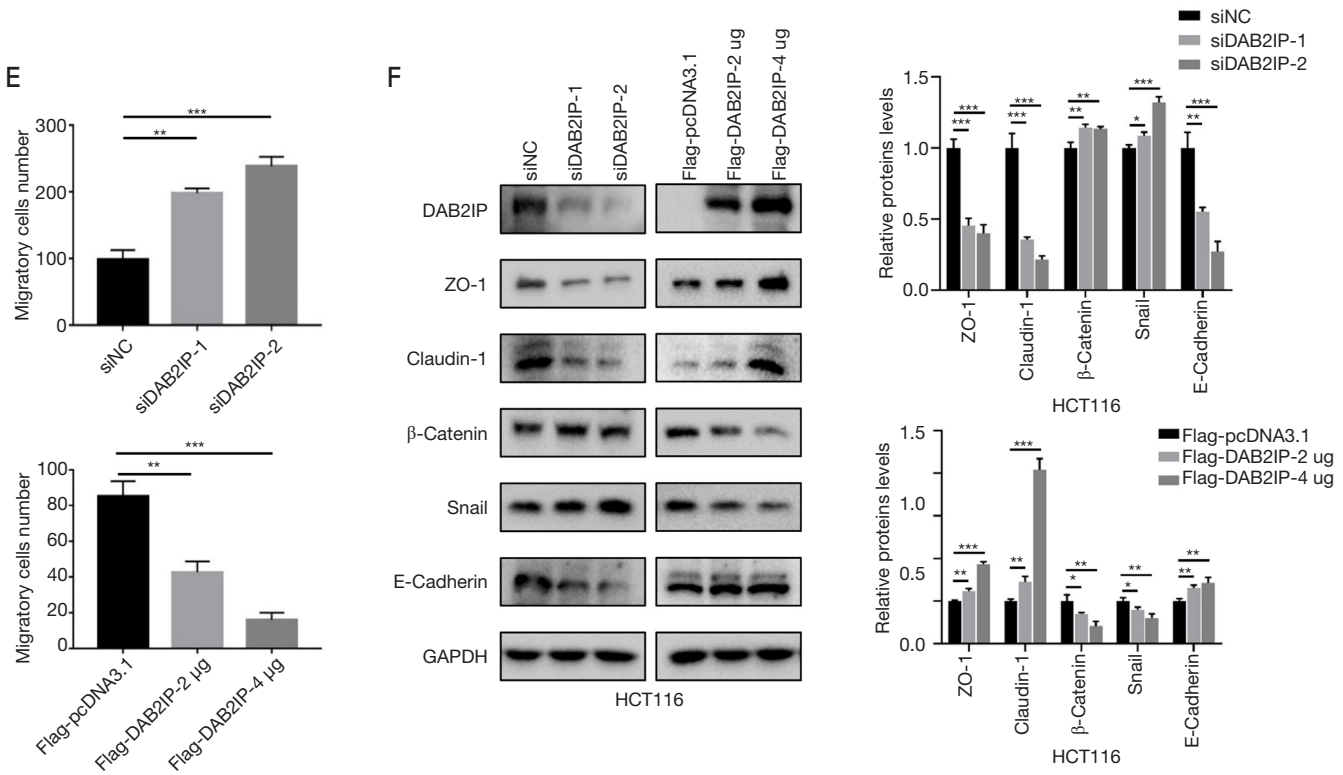

Figure 6 Ectopic DAB2IP inhibits the migration and EMT progress of CRC cells. (A,B) Wound healing assays at different time points measure the effect of DAB2IP on the migration of HCT116 cells transfected with selected siRNAs (siNC, siDAB2IP-1, and siDAB2IP-2) or increased amounts of plasmids (Flag-pcDNA3.1, Flag-DAB2IP-2 μg, and Flag-DAB2IP-4 μg). (C) The quantitative analysis of the migration rates in (A,B), n=3 per group. Scale bar =100 μm. (D) Transwell assays evaluate the migration ability of HCT116 cells transfected with selected siRNAs (siNC, siDAB2IP-1, and siDAB2IP-2) or increased amounts of plasmids (Flag-pcDNA3.1, Flag-DAB2IP-2 μg, and Flag-DAB2IP-4 μg). Representative photographs are presented (magnification ×100, scale bar =100 μm). (E) The relative number of migratory cells are counted as mean ± SEM (n=3). (F) The immunoblotting analysis of ZO-1, Claudin-1, β-catenin, Snail, and E-cadherin expressions in HCT116 cells transfected with selected siRNAs (siNC, siDAB2IP-1, and siDAB2IP-2) or increased amounts of plasmids (Flag-pcDNA3.1, Flag-DAB2IP-2 μg, and Flag-DAB2IP-4 μg) with GAPDH as the loading control. The gray-scale value of straps visually shows the expression of ZO-1, Claudin-1, β-Catenin, Snail and E-Cadherin in HCT116 (Image J software). Error bars represent SEM (n=3). *, P<0.05; **, P<0.01; ***, P<0.001.

In the present study, we demonstrated that the expression of DAB2IP in CRC tissues was notably lower compared with para-cancer tissues by using IHC staining, qRT-PCR and immunoblotting. These results were consistent with data from the Oncomine and GEPIA databases. Given that the mechanism of DAB2IP in CRC has not been fully investigated, we then characterized the expression pattern and correlated the function of DAB2IP in CRC tissues using the publicly available mRNA microarray data sets in GEO. We found that DAB2IP expression was significantly downregulated in CRC tissues and was associated with the cell cycle, DNA replication, and focal adhesion. Moreover, to explore whether DAB2IP is involved in CRC progression, we transiently knocked down or overexpressed DAB2IP in HCT116 cells by transfecting them with siRNAs targeting DAB2IP or plasmids encoding human DAB2IP, respectively. Moreover, our results also revealed that overexpression of DAB2IP significantly inhibited HCT116 cell growth *in vivo* and *in vitro*, accompanied by the downregulation of cyclin D1 and CDK4. Meanwhile, DAB2IP knockdown had reverse effects on the growth of HCT116 cells. These results suggest that DAB2IP plays an essential role in CRC cell progression and tumor formation.

To evaluate whether DAB2IP exerts an influence on

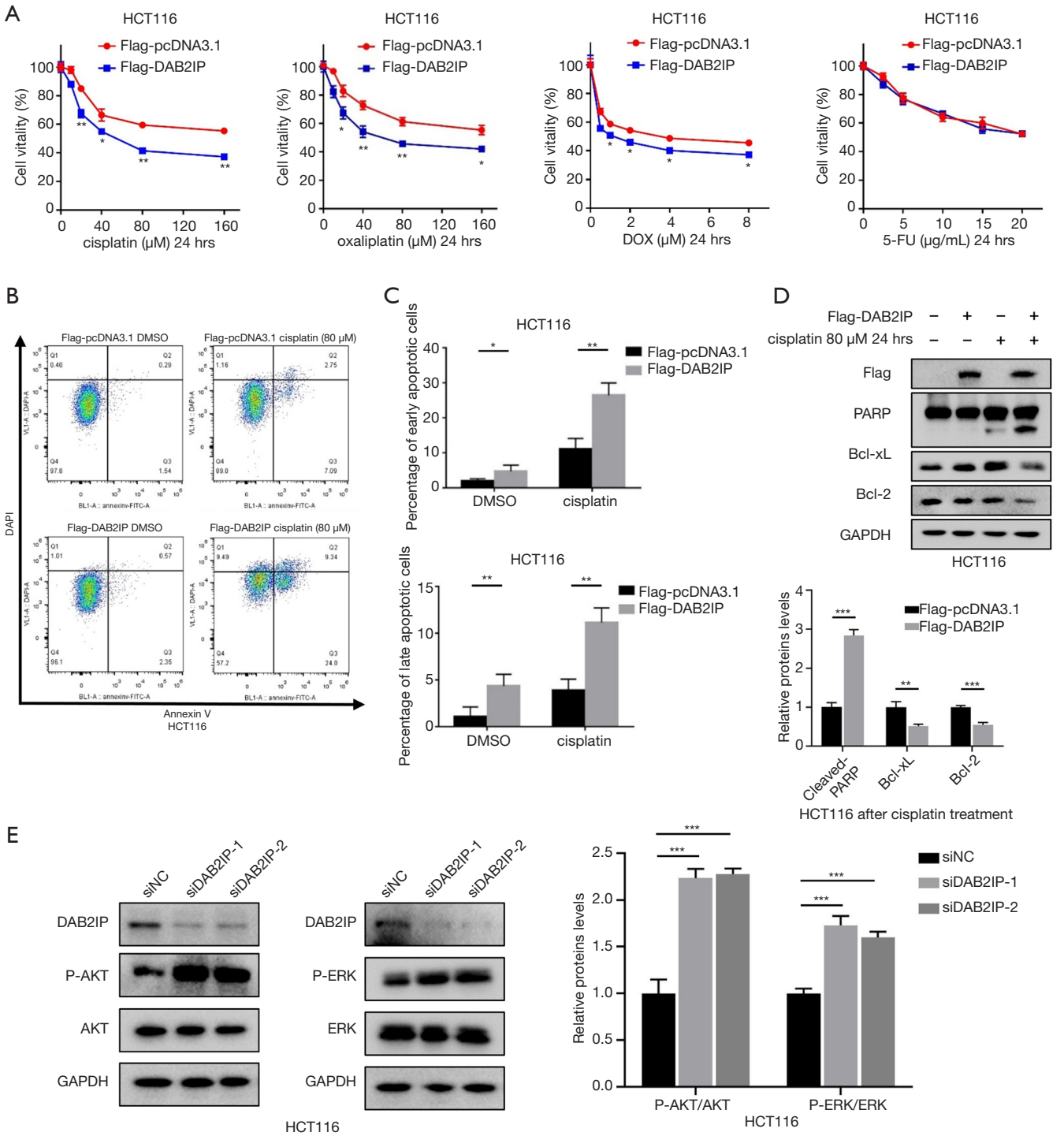

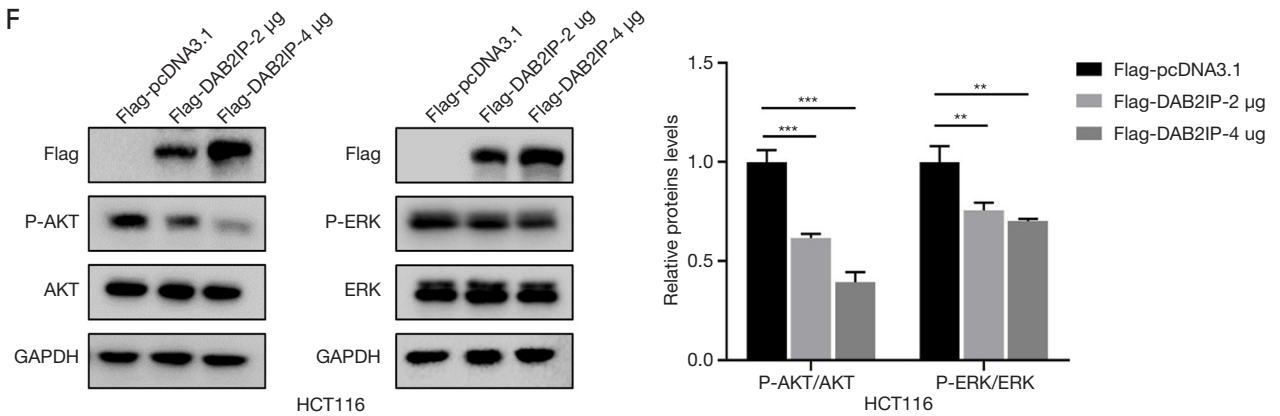

Figure 7 DAB2IP regulates the drug sensitivity of CRC cells to cisplatin, oxaliplatin, and DOX and the intrinsic apoptosis of CRC cells following cisplatin treatment. (A) The CCK-8 assays of HCT116 cell responses to different concentrations of cisplatin, oxaliplatin, doxorubicin (DOX), and 5-fluorouracil (5-FU) after 24 hours. HCT116 cells transfected with Flag-pcDNA3.1 plasmids (Flag-pcDNA3.1) and Flag-DAB2IP-pcDNA3.1 plasmids (Flag-DAB2IP). Results are presented as mean ± SEM (n=8). (B) Cells were transfected with Flag-pcDNA3.1 plasmids (Flag-pcDNA3.1) and Flag-DAB2IP-pcDNA3.1plasmids (Flag-DAB2IP) for 24 hours, then 80 μM cisplatin or DMSO was added, and 24 hours later cells were stained with Annexin V and DAPI, then analyzed by a flow cytometer. (C) The quantitative analysis of apoptotic cells in (B); n=3 per group. (D) Following transfection with selected plasmids expressing Flag-pcDNA3.1 or Flag-DAB2IP-pcDNA3.1 for 36 hours, HCT116 cells were treated with 80 μM of cisplatin or DMSO for 24 hours and then analyzed for the levels of Flag, PARP, Bcl-xL, and Bcl-2 by immunoblotting with GAPDH as the loading control. (E,F) The immunoblotting analysis of P-AKT, AKT, P-ERK, and ERK in HCT116 cells transfected with selected siRNAs (siNC, siDAB2IP-1, and siDAB2IP-2) and increased amounts of plasmids (Flag-pcDNA3.1, Flag-DAB2IP-2 μg, and Flag-DAB2IP-4 μg) with GAPDH as the loading control. The gray-scale value of straps visually shows the expression of Cleaved-PARP, Bcl-xL, Bcl-2, P-AKT and P-ERK in HCT116 (Image J software). Error bars represent SEM (n=3). *, P<0.05; **, P<0.01; ***, P<0.001.

CRC cell growth by regulating the cell cycle, we performed a fluorescence-activated cell sorting (FACS) analysis. Our results showed that after transfection with selected siRNAs, the percentage of HCT116 cells in the G2/M phase was notably higher than that of negative controls, and the percentage of cells in the G0/G1 and S phases was decreased in a certain extent. Meanwhile, overexpression of DAB2IP in HCT116 cells had the opposite effect. In line with this result, our immunoblotting results also showed that knockdown or overexpression of DAB2IP could decrease or increase the expression of P53 and P21. Recent studies suggest that P53-P21 signaling plays a central role in regulating cancer cell growth and arresting the cellular cycle at checkpoints G1/S or G2/M in order to run the repair mechanisms (29,30). Thus, the influence on the CRC cell cycle by the regulation of P53 and P21 caused by DAB2IP may be associated with growth during tumor progression leading to poor prognosis.

Furthermore, the association between DAB2IP and CRC cell migration was observed in our study using wound-healing assays and cell migration assays. Our results showed that compared to the control group, DAB2IP overexpression inhibited the motility of HCT116, and the knockdown of DAB2IP restrained this phenomenon. It is evident that EMT plays a crucial role in tumor cell migration (31). The transdifferentiation of epithelial cells into motile mesenchymal cells, a process known as EMT, is integral in development, wound healing, and stem cell behavior and contributes pathologically to fibrosis and cancer progression (32). In our study, we found a decreased expression of β-Catenin and Snail and an increased expression of ZO-1, Claudin-1, and the EMT marker E-cadherin in HCT116 cells after DAB2IP overexpression. The opposite result was found following DAB2IP knockdown. These results provide an evidence of the effect of DAB2IP on CRC cell EMT progress.

In the current era of new targeted agents and immunotherapy, chemotherapy remains essential in the treatment of most solid malignancies. Understanding the mechanisms of cancer chemoresistance and finding

new ways to enhance the sensitivity of cancer to chemotherapeutic drugs are vital because the majority of cancer cells eventually develop chemoresistance (33). Resistance to chemotherapy is a significant barrier to curing cancer, and multiple molecular mechanisms are involved in chemoresistance. It is well established that cisplatin can induce apoptosis of CRC, and apoptosis has been recognized as a key system that clears aged or damaged cells. It is also essential in the process of carcinogenesis (34). In prostate cancer, DAB2IP loss was reported to confer the resistance of prostate cancer to androgen deprivation therapy by activating STAT3 and inhibiting apoptosis cells (15). Our study showed that overexpression of DAB2IP increased cell sensitivity to cisplatin, oxaliplatin, and DOX but not 5-FU, and we found that upregulation of DAB2IP significantly increased the apoptotic rate of cells compared to negative controls after cisplatin treatment. We also found an association between DAB2IP and several apoptosis-relevant proteins, including Cleaved-PARP, Bcl-2, and Bcl-xL after cisplatin treatment. Our data suggest that targeting DAB2IP as a potential therapeutic strategy may enhance apoptosis induced by chemotherapeutics and heighten the drug sensitivity of CRC cells to cisplatin.

Previous studies have proposed that suppression of DAB2IP occurs in cell lines of different origins engaged in enhancing cell proliferation and migration, and there is a link between decreased DAB2IP and the upregulation of phosphorylated AKT (P-AKT) and phosphorylated ERK (P-ERK) (12,20). In prostate cancer, it was reported that DAB2IP caused the suppression of Egr-1 that is responsible for Clusterin expression, which contributes to chemoresistance (35). In gastric cancer (GC), DAB2IP was reported to regulate GC cell proliferation and chemosensitivity via AKT and ERK signaling (36). In the present study, we further confirmed the inhibitory effect of DAB2IP overexpression on the AKT and ERK signaling pathways in CRC cells. In accordance with the previous studies, we suggest that DAB2IP regulates the growth, migration, EMT of CRC cells and sensitivity to chemotherapeutics by potentially regulating the AKT and ERK signaling pathways.

There are some limitations to our study. Firstly, the role of DAB2IP in CRC cell migration and sensitivity to chemotherapeutic drugs *in vivo* requires further evaluation. Secondly, multicellular tests should be performed to verify the generality of our findings. Moreover, the precise molecular mechanisms of DAB2IP and related signaling pathways remain to be determined. Thus, further research is required to explore the function of DAB2IP in CRC.

In conclusion, we found that overexpression of DAB2IP suppressed CRC progression. Moreover, our results revealed that DAB2IP overexpression inhibited CRC cell growth and migration and sensitized CRC cells to chemotherapeutic drugs. Mechanistically, we found that DAB2IP regulated proteins closely correlated with cell growth, EMT progress, and cell apoptosis. Moreover, inhibition of AKT and ERK may be implicated in the DAB2IP overexpression-mediated increase in sensitivity to chemotherapeutic drugs in CRC. These findings suggest that DAB2IP might be a potential pharmaceutical target for the treatment of CRC.

Acknowledgments

Funding: This work was supported by National Science Foundation (NSF) of Jiangsu Province of China (BK20191172; SH), Project of Key Laboratory of Clinical Pharmacy of Jiangsu Province of China (XZSYSKF2020027; GZ), Project of Gusu Medical Key Talent of Suzhou City of China (GSWS2020005; SH), Project of New Pharmaceutics and Medical Apparatuses of Suzhou City of China (SLJ2021007; SH), Project of Science and Technology Plan of Suzhou of China (SYS2019050; LS) and Project of Science and Technology Development Plan of Suzhou City of China (SYS2019007; GZ).

Footnote

Reporting Checklist: The authors have completed the ARRIVE reporting checklist. Available at https://dx.doi.org/10.21037/atm-21-3474

Data Sharing Statement: Available at https://dx.doi.org/10.21037/atm-21-3474

Conflicts of Interest: All authors have completed the ICMJE uniform disclosure form (available at https://dx.doi.org/10.21037/atm-21-3474). YY reports the leadership or fiduciary role in Review Board of Animal Care and Use of Suzhou Institute of Systems Medicine (Suzhou, China); SH reports funding support from National Science Foundation (NSF) of Jiangsu Province of China (BK20191172; SH), and the leadership or fiduciary role in Ethics and Research Committee of the First Affiliated Hospital of Soochow University (Suzhou, China); GZ reports funding support from the Project of Key Laboratory of Clinical Pharmacy of Jiangsu Province of China (XZSYSKF2020027; GZ); SH

reports Project of Gusu Medical Key Talent of Suzhou City of China (GSWS2020005; SH); SH reports Project of New Pharmaceutics and Medical Apparatuses of Suzhou City of China (SLJ2021007; SH); LS reports Project of Science and Technology Plan of Suzhou of China (SYS2019050; LS); GZ reports Project of Science and Technology Development Plan of Suzhou City of China (SYS2019007; GZ). The other authors have no conflicts of interest to declare.

Ethical Statement: The authors are accountable for all aspects of the work in ensuring that questions related to the accuracy or integrity of any part of the work are appropriately investigated and resolved. All procedures performed in this study involving human participants were in accordance with the Declaration of Helsinki (as revised in 2013). The study was approved by Biomedical Research Ethics Committee of the First Affiliated Hospital of Soochow University (Suzhou, China) (2021-NO:177) and informed consent was taken from all the patients. Experiments were performed under a project license (No. ISM-IACUC-0054-R) granted by Animal Ethics Committee of Suzhou Institute of Systems Medicine (Suzhou, China), in compliance with institutional guidelines for the care and use of animals.

References

1. Brody H. Colorectal cancer. Nature 2015;521:S1.
2. Bray F, Ferlay J, Soerjomataram I, et al. Global cancer statistics 2018: GLOBOCAN estimates of incidence and mortality worldwide for 36 cancers in 185 countries. CA Cancer J Clin 2018;68:394-424.
3. Arnold M, Sierra MS, Laversanne M, et al. Global patterns and trends in colorectal cancer incidence and mortality. Gut 2017;66:683-91.
4. Fidler MM, Bray F, Vaccarella S, et al. Assessing global transitions in human development and colorectal cancer incidence. Int J Cancer 2017;140:2709-15.
5. GBD 2017 Colorectal Cancer Collaborators. The global, regional, and national burden of colorectal cancer and its attributable risk factors in 195 countries and territories, 1990-2017: a systematic analysis for the Global Burden of Disease Study 2017. Lancet Gastroenterol Hepatol 2019;4:913-33. Erratum in: Lancet Gastroenterol Hepatol 2020;5:e2.
6. Kopetz S. New therapies and insights into the changing landscape of colorectal cancer. Nat Rev Gastroenterol Hepatol 2019;16:79-80.
7. Yi H, Liao ZW, Chen JJ, et al. Genome variation in colorectal cancer patient with liver metastasis measured by whole-exome sequencing. J Gastrointest Oncol 2021;12:507-15.
8. Kong Z, Raghavan P, Xie D, et al. Epothilone B confers radiation dose enhancement in DAB2IP gene knock-down radioresistant prostate cancer cells. Int J Radiat Oncol Biol Phys 2010;78:1210-8.
9. Shen YJ, Kong ZL, Wan FN, et al. Downregulation of DAB2IP results in cell proliferation and invasion and contributes to unfavorable outcomes in bladder cancer. Cancer Sci 2014;105:704-12.
10. Zhang X, Li N, Li X, et al. Low expression of DAB2IP contributes to malignant development and poor prognosis in hepatocellular carcinoma. J Gastroenterol Hepatol 2012;27:1117-25.
11. Xie D, Gore C, Liu J, et al. Role of DAB2IP in modulating epithelial-to-mesenchymal transition and prostate cancer metastasis. Proc Natl Acad Sci U S A 2010;107:2485-90.
12. Sun L, Yao Y, Lu T, et al. DAB2IP Downregulation Enhances the Proliferation and Metastasis of Human Gastric Cancer Cells by Derepressing the ERK1/2 Pathway. Gastroenterol Res Pract 2018;2018:2968252.
13. Wang J, Zhu X, Hu J, et al. The positive feedback between Snail and DAB2IP regulates EMT, invasion and metastasis in colorectal cancer. Oncotarget 2015;6:27427-39.
14. Dai X, North BJ, Inuzuka H. Negative regulation of DAB2IP by Akt and SCFFbw7 pathways. Oncotarget 2014;5:3307-15.
15. Zhou J, Ning Z, Wang B, et al. DAB2IP loss confers the resistance of prostate cancer to androgen deprivation therapy through activating STAT3 and inhibiting apoptosis. Cell Death Dis 2015;6:e1955.
16. Zhang H, Zhang R, Luo Y, et al. AIP1/DAB2IP, a novel member of the Ras-GAP family, transduces TRAF2-induced ASK1-JNK activation. J Biol Chem 2004;279:44955-65.

17. Zhu XH, Wang JM, Yang SS, et al. Down-regulation of DAB2IP promotes colorectal cancer invasion and metastasis by translocating hnRNPK into nucleus to enhance the transcription of MMP2. Int J Cancer 2017;141:172-83.
18. Min J, Liu L, Li X, et al. Absence of DAB2IP promotes cancer stem cell like signatures and indicates poor survival outcome in colorectal cancer. Scientific reports 2015;5:16578.
19. Rebillard A, Jouan-Lanhouet S, Jouan E, et al. Cisplatin-induced apoptosis involves a Fas-ROCK-ezrin-dependent actin remodelling in human colon cancer cells. Eur J Cancer 2010;46:1445-55.
20. Xie D, Gore C, Zhou J, et al. DAB2IP coordinates both PI3K-Akt and ASK1 pathways for cell survival and apoptosis. Proc Natl Acad Sci U S A 2009;106:19878-83.
21. Dote H, Toyooka S, Tsukuda K, et al. Aberrant promoter methylation in human DAB2 interactive protein (hDAB2IP) gene in breast cancer. Clin Cancer Res 2004;10:2082-9.
22. Yano M, Toyooka S, Tsukuda K, et al. Aberrant promoter methylation of human DAB2 interactive protein (hDAB2IP) gene in lung cancers. Int J Cancer 2005;113:59-66.
23. Duan Y, Yin X, Lai X, et al. Upregulation of DAB2IP Inhibits Ras Activity and Tumorigenesis in Human Pancreatic Cancer Cells. Technol Cancer Res Treat 2020;19:1533033819895494.
24. Wang B, Huang J, Zhou J, et al. DAB2IP regulates EMT and metastasis of prostate cancer through targeting PROX1 transcription and destabilizing HIF1α protein. Cell Signal 2016;28:1623-30.
25. Yun EJ, Baek ST, Xie D, et al. DAB2IP regulates cancer stem cell phenotypes through modulating stem cell factor receptor and ZEB1. Oncogene 2015;34:2741-52.
26. Kong Z, Xie D, Boike T, et al. Downregulation of human DAB2IP gene expression in prostate cancer cells results in resistance to ionizing radiation. Cancer Res 2010;70:2829-39.
27. Yu L, Tumati V, Tseng SF, et al. DAB2IP regulates autophagy in prostate cancer in response to combined treatment of radiation and a DNA-PKcs inhibitor. Neoplasia 2012;14:1203-12.
28. Yuan SP, Li CX, Qin S, et al. High expression of disabled homolog 2-interacting protein contributes to tumor development and proliferation in cutaneous squamous cell carcinoma. Ann Transl Med 2020;8:1131.
29. Engeland K. Cell cycle arrest through indirect transcriptional repression by p53: I have a DREAM. Cell Death Differ 2018;25:114-32.
30. Sancar A, Lindsey-Boltz LA, Unsal-Kaçmaz K, et al. Molecular mechanisms of mammalian DNA repair and the DNA damage checkpoints. Annu Rev Biochem 2004;73:39-85.
31. Gonzalez DM, Medici D. Signaling mechanisms of the epithelial-mesenchymal transition. Sci Signal 2014;7:re8.
32. Lamouille S, Xu J, Derynck R. Molecular mechanisms of epithelial-mesenchymal transition. Nat Rev Mol Cell Biol 2014;15:178-96.
33. Yao Y, Yang X, Sun L, et al. Fatty acid 2-hydroxylation inhibits tumor growth and increases sensitivity to cisplatin in gastric cancer. EBioMedicine 2019;41:256-67.
34. Taylor RC, Cullen SP, Martin SJ. Apoptosis: controlled demolition at the cellular level. Nat Rev Mol Cell Biol 2008;9:231-41.
35. Wu K, Xie D, Zou Y, et al. The mechanism of DAB2IP in chemoresistance of prostate cancer cells. Clin Cancer Res 2013;19:4740-9.
36. Wang G, Wang X, Han M, et al. Loss of DAB2IP Contributes to Cell Proliferation and Cisplatin Resistance in Gastric Cancer. Onco Targets Ther 2021;14:979-88.

(English Language Editor: D. Fitzgerald)

Cite this article as: Wu G, Xu X, Wan D, Zhou D, Feng Y, Chen J, Peng Z, Fang D, Shi X, Yao H, Chen G, Sun L, Yao Y, Zhou G, Yang Y, He S. DAB2IP decreases cell growth and migration and increases sensitivity to chemotherapeutic drugs in colorectal cancer. Ann Transl Med 2021;9(16):1317. doi: 10.21037/atm-21-3474

